Published in final edited form as:

Mol Cancer Ther. 2017 September ; 16(9): 1979–1988. doi:10.1158/1535-7163.MCT-17-0032.

FBW7-dependent Mcl-1 degradation mediates the anticancer effect of Hsp90 inhibitors

Jingshan Tong[1,2,#], **Shuai Tan**[1,2,3,#], **Zaneta Nikolovska-Coleska**[4], **Jian Yu**[1,5], **Fangdong Zou**[3,*], and **Lin Zhang**[1,2,*]

[1]University of Pittsburgh Cancer Institute, University of Pittsburgh School of Medicine, Pittsburgh, PA, 15213

[2]Department of Pharmacology and Chemical Biology, University of Pittsburgh School of Medicine, Pittsburgh, PA, 15213

[3]College of Life Sciences, Sichuan University, Chengdu, Sichuan, 610064, P.R. China

[4]Department of Pathology, University of Michigan Medical School, Ann Arbor, MI, USA

[5]Department of Pathology, University of Pittsburgh School of Medicine, Pittsburgh, PA, 15213, USA

Abstract

Heat shock protein 90 (Hsp90) is widely overexpressed in cancer cells and necessary for maintenance of malignant phenotypes. Hsp90 inhibition induces tumor cell death through degradation of its client oncoproteins, and has shown promises in preclinical studies. However, the mechanism by which Hsp90 inhibitors kill tumor cells is not well understood. Biomarkers associated with differential sensitivity and resistance to Hsp90 inhibitors remain to be identified. In this study, we found that colorectal cancer (CRC) cells containing inactivating mutations of *FBW7*, a tumor suppressor and E3 ubiquitin ligase, are intrinsically insensitive to Hsp90 inhibitors. The insensitive CRC cells lack degradation of Mcl-1, a pro-survival Bcl-2 family protein. Hsp90 inhibition promotes GSK3β-dependent phosphorylation of Mcl-1, which subsequently binds to FBW7 and undergoes ubiquitination and proteasomal degradation. Specifically blocking Mcl-1 phosphorylation by genetic knock-in abrogates its degradation and renders *in vitro* and *in vivo* resistance to Hsp90 inhibitors, which can be overcame by Mcl-1-selective small-molecule inhibitors. Collectively, our findings demonstrate a key role of GSK3β/FBW7-dependent Mcl-1 degradation in killing of CRC cells by Hsp90 inhibitors, and suggest *FBW7* mutational status as a biomarker for Hsp90-targeted therapy.

Keywords

Hsp90 inhibitors; Mcl-1; FBW7; colon cancer; apoptosis

[*]**Corresponding authors:** Lin Zhang, the UPCI Research Pavilion, Room 2.42a, Hillman Cancer Center, 5117 Centre Ave., Pittsburgh, PA 15213, USA. Phone: (412) 623-1009. Fax: (412) 623-7778. zhanglx@upmc.edu; Fangdong Zou, College of Life Sciences, Sichuan University, Chengdu, Sichuan, 610064, P.R. China; Phone: +86-28-85412805. Fax: +86-28-85412805. fundzou@scu.edu.cn.

[#]These authors contribute equally to this work.

Introduction

Heat shock protein 90 (Hsp90) is a molecular chaperone that mediates the stability and function of a variety of client proteins involved in cell proliferation and survival (1). Hsp90 is constitutively overexpressed in a variety types of cancers (2). Among over 200 Hsp90 client proteins identified, many are oncoproteins associated with hallmarks of cancer (3), such as mutant p53, Raf-1, and Akt (2), suggesting that it represents an attractive target for developing new anticancer therapy.

A number of small-molecule Hsp90 inhibitors have been developed (4, 5). Most of these inhibitors, including the natural product geldanamycin and its derivative 17-allylamino-17-demethoxygeldanamycin 17-AAG; telatinib), bind to the amino-terminal ATP-binding pocket of Hsp90 and disrupt its complex formation with client proteins (2, 6). Inhibitors for targeting the carboxyl-terminal binding sites of Hsp90 have also been identified (7, 8). Over 17 Hsp90 inhibitors have entered phase I/II clinical trials, such as 17-AAG and its analog 17-DMAG 17-Dimethylaminoethylamino-17-demethoxygeldanamycin; Alvespimycin) with improved pharmaceutical properties (2, 5). Previous studies showed that geldanamycin and 17-AAG induce apoptosis and inhibit tumor metastasis and angiogenesis (2, 9). Several anticancer mechanisms of Hsp90 inhibitors have been proposed, such as downregulation of Akt (10), inhibition of NF-kB activation due to IKK destabilization (11), endoplasmic reticulum stress (12), and more recently, activation of p53 and its downstream targets (13–15). However, the mechanisms by which Hsp90 inhibitors selectively kill tumor cells are still not well understood. Biomarkers associated with differential sensitivity and resistance to Hsp90 inhibitors remain to be identified.

Apoptosis in mammalian cells is governed by the Bcl-2 family proteins via a cascade of cellular events, including permeabilization of outer mitochondrial membrane, release of the mitochondrial proteins such as cytochrome *c*, and activation of caspases (16, 17). Myeloid cell leukemia 1 (Mcl-1) is a pro-survival Bcl-2 family member frequently overexpressed or amplified in various human tumors (18). Mcl-1 suppresses apoptosis by binding to the BH3 domains of pro-apoptotic proteins through a surface groove containing hydrophobic pockets (16). Distinctive from other Bcl-2 members, Mcl-1 is quite unstable and has a short half-life (19). Defective Mcl-1 degradation allows tumor cells to evade death and become resistant to anticancer therapies. Recent studies identified F-box/WD repeat containing protein 7 (FBW7) as an E3 ubiquitin ligase that targets phosphorylated Mcl-1 through glycogen synthase kinase 3β (GSK3β) for destruction (20, 21). *FBW7* (*FBXW7*; *CDC4*) is a tumor suppressor frequently mutated in human cancers, including 10–20% of colorectal tumors (22, 23). Heterozygous FBW7 missense mutations are often detected in three arginine residues (R465, R479 and R505), which are critical for binding to a conserved CDC4 phosphodegron motif of its substrates (23).

In this study, we identified a critical role of GSK3β/FBW7-mediated Mcl-1 degradation in apoptosis induced by Hsp90 inhibitors in CRC cells. Importantly, colorectal cancer (CRC) cells containing *FBW7* mutations are insensitive to Hsp90 inhibitors due to blocked Mcl-1 degradation. Our results suggest *FBW7* mutational status as a potential biomarker, and the use of Mcl-1-selective inhibitors for overcoming resistance to Hsp90-targeted therapy.

Materials and Methods

Cell culture

Human CRC cell lines, including HCT116, DLD1, RKO, LoVo, Lim2405, SW48, and HCT-8 were obtained from the American Type Culture Collection (Manassas, VA). Isogenic *FBW7*-KO HCT116 and DLD1 cell lines were obtained from Horizon Discovery (Cambridge, UK) (22). HCT116 cells with knock-in of the Mcl-1 phosphorylation site mutant S121A/E125A/S159A/T163A (*Mcl-1*-KI) were generated by homologous recombination as described (24). Cells were authenticated by genotyping and analysis of protein expression by western blotting throughout the study, and routinely checked for Mycoplasma contamination by PCR. All cell lines were maintained at 37°C in 5% CO_2 and cultured in McCoy's 5A modified media (Invitrogen) supplemented with 10% defined FBS (HyClone), 100 units/ml penicillin, and 100 μg/ml streptomycin (Invitrogen). For drug treatment, cells were plated in 12-well plates at 20–30% density 24 hr before treatment. DMSO (Sigma) stocks of agents, including 17-AAG, 17-DMAG, MG132, TW-37, SB216763 (25) (Selleck Chemicals), 5-fluorouracil (5-FU; Sigma), necrosulfonamide (NSA) (Calbiochem), and Mcl-1 inhibitors including UMI-77 (26), UMI-212 (compound **21**) and UMI-36 (compound **36**) (27), were diluted to appropriate concentrations with cell culture medium.

MTS assay

Cells seeded in 96-well plates at a density of 1×10^4 cells/well were treated with 17-AAG or 17-DMAG for 72 hr. 3-(4, 5-dimethylthiazol-2-yl)-5-(3-carboxymethoxyphenyl)-2-(4-sulfophenyl)-2H-tetrazolium (MTS) assay was performed using the MTS assay kit (Promega) according to the manufacturer's instructions. Chemiluminescence was measured by a Wallac Victor 1420 Multilabel Counter (Perkin Elmer). Each assay was conducted in triplicate and repeated three times.

Western blotting

Western blotting was performed as previously described (28), with antibodies for phospho-Mcl-1 (Ser159/Thr163), cleaved caspases 3, 8, and 9, ERK, phospho-ERK (Thr202/Tyr204), AKT, phospho-AKT (Ser473), GSK3β, phospho-GSK3β (Ser9) (Cell Signaling), cytochrome oxidase subunit IV (Invitrogen), HA (Santa Cruz), Mcl-1 (BD Biosciences), β-actin, cytochrome *c*, Flag (Sigma), p62 (Novus), LC3 (MBL), and FBW7 (Abcam).

Transfection and siRNA knockdown

WT *FBW7* expression construct was a gift from Dr. Wenyi Wei at Harvard Medical School. Mutant *FBW7* and HA-ubiquitin expression constructs were previously described (24, 29). Transfection was performed using Lipofectamine 2000 (Invitrogen) according to the manufacturer's instructions. siRNA transfection was done 24 hr before drug treatment using 200 pmol of control scrambled siRNA, human *Mcl-1* siRNA (CGCCGAATTCATTAATTTATT-dTdT) (GE Dharmacon), or human *GSK3β* siRNA (sc-35527; Santa Cruz).

Immunoprecipitation

After treatment, cells were harvested and re-suspended in 1 ml of EBC buffer (50 mM Tris-HCl, pH 7.5, 100 mM NaCl, 0.5% Nonidet P–40) supplemented with a protease inhibitor cocktail (Roche). Cell suspensions were sonicated and spun at 10,000×g for 10 min to prepare cell lysates. For immunoprecipitation (IP), 1–2 μg of IP antibodies were mixed with protein G/A-agarose beads (Invitrogen) for 20 min at room temperature. The beads were washed twice with PBS containing 0.02% Tween 20 (pH 7.4), incubated with cell lysates on a rocker for 6 hr at room temperature, and then washed three times with PBS (pH 7.4). Beads were then boiled in 2× Laemmli buffer and subjected to SDS-PAGE and western blot analysis.

Reverse transcriptase (RT) PCR and genomic PCR

Total RNA was isolated using the Mini RNA Isolation II kit (ZYMO Research) according to the manufacturer's protocol. One-μg of total RNA was used to generate cDNA by the SuperScript II reverse transcriptase (Invitrogen). Real-time PCR was carried out for *Mcl-1* using the primer pair 5'-ATGCTTCGGAAACTGGACAT-3'/5'-TGGAAGAACTCCACAAACCCA-3'; and for *β-actin* using the primer pair 5'-GACCTGACAGACTACCTCAT-3'/5'-AGACAGCACTGTGTTGGCTA-3' as described (30).

Analysis of apoptosis

Apoptosis was measured by counting condensed and fragmented nuclei after nuclear staining with Hoechst 33258 (Invitrogen) as previously described (30). At least 300 cells were analyzed for each sample. Colony formation assays were performed by plating treated cells in 12-well plates at appropriate dilutions, followed by crystal violet staining 14 days after plating as described (30). Each experiment was performed in triplicate and repeated at least twice. Cytochrome *c* release was analyzed by western blotting of cytoplasmic and mitochondrial fractions isolated from treated cells as described (28).

Xenograft tumor experiments

The described animal experiments were approved by the University of Pittsburgh Institutional Animal Care and Use Committee. Female 5- to 6-week-old Nu/Nu mice (Charles River) were housed in micro isolator cages in a sterile environment, and allowed access to water and chow *ad libitum*. Xenograft tumors were established by subcutaneously injecting mice with 4×10^6 of each cell line. After tumor growth for 7 days, mice were treated daily on days 1-4 and 7-11 with 17-DMAG (15 mg/kg/d) or the control vehicle. Tumor volumes were measured by calipers and calculated according to the formula $0.5 \times \text{length} \times \text{width}^2$. After mice tumors reached 1.0 cm^3 in size, mice were euthanized and tumors were dissected and fixed in 10% formalin and embedded in paraffin. Terminal deoxynucleotidyl transferase mediated dUTP Nick End Labeling (TUNEL; Millipore) and active caspase-3 (Cell Signaling) immunostaining was performed on 5-mm paraffin-embedded tumor sections as previously described (28). Signals were detected by Alexa Fluor 488- (for TUNEL) or Alexa Fluor 594-conjugated (for active caspase-3) secondary

antibodies (Invitrogen) with nuclear counter staining by DAPI (4' 6-Diamidino-2-phenylindole).

Statistical Analysis

Statistical analysis was carried out using GraphPad Prism IV software. *P* values were calculated by the student's t-test and were considered significant if $P < 0.05$. Means ± one standard deviation (s.d.) were displayed in the figures.

Results

CRC cells containing *FBW7* mutations are insensitive to Hsp90 inhibitors and lack Mcl-1 degradation

Upon analyzing CRC cell lines with different mutations in common tumor suppressors and oncogenes, we identified a correlation between 17-AAG sensitivity and *FBW7* mutational status (Supplementary Table S1). *FBW7*-mutant CRC cell lines, including SW48, HCT-8, and LoVo, were substantially less sensitive to 17-AAG, compared to *FBW7*-wild-type (WT) cell lines, including RKO, HCT116, Lim2405 (Fig. 1A). The IC_{50} of 17-AAG ranged from 1.28–3.07 μM in the *FBW7*-mutant cell lines, compared to 0.30–0.46 μM in the WT cell lines (Supplementary Table S1). Compared with WT cells, *FBW7*-mutant cells had lower levels of 17-AAG-induced apoptosis determined by nuclear fragmentation (Fig. 1B). Analysis of the expression of Bcl-2 family proteins revealed marked depletion of the antiapoptotic Mcl-1 in WT cells, but not in *FBW7*-mutant cells (Fig. 1C and D). In contrast, proapoptotic members, including PUMA, Bax, and Bim, were similarly upregulated in *FBW7*-WT and -mutant CRC cells (15) (Supplementary Fig. S1). These results demonstrate that *FBW7* mutations are associated with blocked Mcl-1 depletion and apoptosis in response to Hsp90 inhibition in CRC cells.

FBW7 is critical for 17-AAG sensitivity and Mcl-1 degradation in CRC cells

To investigate the role of *FBW7* in regulating sensitivity to Hsp90 inhibitors, we analyzed isogenic HCT116 cells with knockout (KO) of *FBW7* (*FBW7*-KO) (22). Compared to the parental cells, *FBW7*-KO HCT116 cells were substantially more resistant to apoptosis induced by 17-AAG (Fig. 2A), and were deficient in 17-AAG-induced Mcl-1 degradation (Fig. 2B). Similar results were obtained with another Hsp90 inhibitor, 17-DMAG (Fig. 2A and B). Reconstituting WT *FBW7* expression in *FBW7*-KO cells by transient transfection restored 17-AAG sensitivity, as well as Mcl-1 degradation (Fig. 2C). Knocking down *Mcl-1* by siRNA also restored 17-AAG sensitivity in *FBW7*-KO cells (Fig. 2C). Similar observations were made using WT and *FBW7*-KO DLD1 cells (22) (Supplementary Fig. S2A–C). Furthermore, transfection of WT *FBW7*, which did not affect the expression of mutant FBW7 (Supplementary Fig. S2D), and *Mcl-1* knockdown also restored 17-AAG sensitivity and apoptosis induction in *FBW7*-mutant SW48 cells (Fig. 2D). In contrast to WT *FBW7*, transfection with tumor-derived *FBW7* mutants, including R465C, R479Q and R505C, failed to restore 17-AAG sensitivity and Mcl-1 degradation in SW48 and *FBW7*-KO HCT116 and DLD1 cells (Fig. 2E; Supplementary Fig. S2E and F). These results demonstrate that the functional *FBW7* is required for 17-AAG sensitivity and Mcl-1

degradation in CRC cells, and that *FBW7* inactivating mutations abrogate Mcl-1 degradation and apoptosis in response to Hsp90 inhibition.

Hsp90 inhibition induces GSK3β-dependent Mcl-1 phosphorylation, which mediates its interaction with FBW7 and proteasomal degradation

We investigated the mechanism by which Hsp90 inhibitors induce FBW7-dependent Mcl-1 depletion. Treating the sensitive HCT116 cells with 17-AAG or 17-DMAG caused Mcl-1 depletion in a time- and dose-dependent manner (Fig. 1C; Supplementary Fig. S3A and B), and did not significantly affect the mRNA level of *Mcl-1* (Supplementary Fig. S3C). 17-AAG-induced Mcl-1 depletion was blocked by the proteasome inhibitor MG132 (Fig. 3A), suggesting ubiquitin/proteasome-dependent protein degradation. In 17-AAG-treated cells, we detected phosphorylation of Mcl-1 at Ser159/Thr163 (Fig. 3B), binding of phosphorylated Mcl-1 (p-Mcl-1) to FBW7 (Fig. 3C), and ubiquitination of Mcl-1 (Fig. 3D), which was dependent on FBW7 and completely blocked in *FBW7*-KO cells (Fig. 3D).

GSK3β was previously shown to phosphorylate Mcl-1 to promote its degradation (31), and is inhibited by ERK through Ser9 phosphorylation (32). Analysis of upstream kinase signaling revealed that 17-AAG prevented Ser9 phosphorylation of GSK3β and inhibited ERK activity (Fig. 3B). Treating cells with the GSK3 inhibitor SB216763 (25) suppressed 17-AAG-induced Mcl-1 phosphorylation, binding to FBW7, ubiquitination and degradation (Fig. 3E and F), which was verified by knocking down *GSK3β* using siRNA (Supplementary Fig. S3D). These results suggest that Hsp90 inhibitors promote GSK3β-dependent Mcl-1 phosphorylation, which facilitates its binding to FBW7 and subsequent ubiquitination and proteasomal degradation.

Blocking Mcl-1 phosphorylation suppresses 17-AAG-induced Mcl-1 degradation and apoptosis

To determine the functional role of Mcl-1 degradation in apoptotic response to Hsp90 inhibitors, we sought to specifically inhibit Mcl-1 phosphorylation and degradation by a genetic approach. A knock-in (KI) strategy was used to target the phosphorylation sites of Mcl-1 involved in its degradation, including S121, S125, S159 and T163 (Fig. 4A), which have been shown to be phosphorylated by GSK3β and other kinases in response to therapeutic agents and other stresses (20, 21). HCT116 cell lines with KI of Mcl-1 phosphorylation site mutant (*Mcl-1*-KI) were identified (Fig. 4A) (24). In stark contrast to WT cells, *Mcl-1*-KI cells were deficient in 17-AAG- and 17-DMAG-induced Mcl-1 degradation (Fig. 4B), and completely lacked Mcl-1 phosphorylation, binding to FBW7, and ubiquitination (Fig. 4, C and D).

Mcl-1-KI cells were markedly resistant to 17-AAG and 17-DMAG, showing significantly increased viability (Fig. 5A), reduced apoptosis (Fig. 5B), and enhanced clonogenic survival (Fig. 5C), upon 17-AAG or 17-DMAG treatment. *Mcl-1*-KI and *GSK3β*-knockdown cells had reduced activation of caspases 9 and 3 (Fig. 5D and Supplementary Fig. S3D) and cytosolic release of cytochrome *c* (Fig. 5E), hallmarks of mitochondria-mediated apoptosis (33). The effect is *Mcl-1*-dependent, as knockdown of *Mcl-1* restored apoptosis induced by 17-AAG and 17-DMAG in *Mcl-1*-KI cells (Fig. 5B). In contrast to apoptosis inhibition,

necroptosis and autophagy induced by anticancer agents, such as 5-fluorouracil (5-FU), was not affected in *Mcl-1*-KI cells (Supplementary Fig. S4A and B). Furthermore, treating cells with an Mcl-1-selective small-molecule inhibitor and analogs, including UMI-77 (26), UMI-212 (compound **21**) and UMI-36 (compound **36**) (27), or the pan-Bcl-2 inhibitor TW-37 with strong Mcl-1 inhibitory activity (34), restored 17-AAG- and 17-DMAG-induced apoptosis in both *FBW7*-KO and *Mcl-1*-KI cells (Fig. 5F), suggesting that inhibiting Mcl-1 overcomes resistance to Hsp90 inhibitors in CRC cells.

FBW7 and Mcl-1 degradation contribute to the *in vivo* antitumor effects of Hsp90 inhibition

We then used xenograft model to validate the role of *FBW7* and Mcl-1 phosphorylation and degradation in Hsp90-targeted therapy. Xenograft tumors were established by subcutaneously injecting nude mice with WT, *Mcl-1*-KI and *FBW7*-KO HCT116 cells. After tumor establishment, tumor-bearing mice were IP injected with 15 mg/kg of water-soluble 17-DMAG or the control vehicle, followed by analysis of tumor size every 2 days for 3 weeks. WT tumors responded well to 17-DMAG treatment, and were only ~1/4 of the size of vehicle-treated tumors on day 21 (Fig. 6, A and B). In contrast, *Mcl-1*-KI and *FBW7*-KO HCT116 tumors were significantly more resistant to 17-DMAG treatment (Fig. 6, A and B). 17-DMAG-treated *Mcl-1*-KI and *FBW7*-KO tumors showed blocked Mcl-1 depletion but with intact GSK3β de-phosphorylation (Fig. 6C). Apoptosis was significantly reduced in the *Mcl-1*-KI and *FBW7*-KO tumors compared to WT tumors as shown by TUNEL and active caspase 3 staining (Fig. 6, D and E). Together, these findings demonstrate a critical role of FBW7 in mediating the *in vivo* antitumor effects of Hsp90 inhibition via the degradation of phosphorylated Mcl-1.

Discussion

Inhibition of Hsp90, which buffers various stresses incurred by oncogenic transformation, promotes degradation of oncogenic client proteins and death of tumor cells (2, 3). Our results demonstrate for the first time that the apoptotic response to Hsp90 inhibitors is mediated by GSK3β/FBW7-dependent Mcl-1 degradation both *in vitro* and *in vivo*. Results from isogenic knock-in cells indicate that the four phosphorylation sites (S121/E125 /S159/T163) are essential for Mcl-1 ubiquitination and degradation induced by Hsp90 inhibitors. Phosphorylation at these sites by GSK3β engages Mcl-1 to bind to FBW7, which likely recruits Mcl-1 to the SCF ubiquitin ligase complex composing of FBW7, CUL1, SKP1 and ROC1 (21). This complex then covalently links ubiquitin chains to Mcl-1, leading to its degradation in the 26S proteasome. In addition to GSK3β, several other kinases have also been implicated in regulating Mcl-1 turnover, including p38, JNK, CDK1, and casein kinase II (20, 21, 31). Mcl-1 stability can also be regulated by other E3 ubiquitin ligases such as Mule and β-TrCP (35, 36), and by the deubiquitinase USP9X (37). Depending on cell types, these proteins may also be involved in modulating sensitivity to Hsp90 inhibitors through their effect on Mcl-1 stability. Furthermore, siRNA screen identified the E3 ubiquitin ligase Cullin-5 as a mediator of response to Hsp90 inhibitors (38).

Unlike in hematopoietic cells, which are dependent on Mcl-1 for survival, depletion of Mcl-1 alone in CRC and most solid tumor cells is not sufficient for inducing cell death. Our

recent study showed that the induction of the proapoptotic Bcl-2 family member PUMA by p53 is also a key event in apoptotic response to Hsp90 inhibitors in CRC cells (15). Mcl-1 binds to and sequesters BH3-only Bcl-2 family proteins to suppress apoptosis (18). It is possible that Mcl-1 degradation induced by Hsp90 inhibitors primarily exerts an effect on PUMA by reliving its full pro-apoptotic activity. In *Mcl-1*-KI and *FBW7*-mutant CRC cells with defective Mcl-1 degradation, Mcl-1 may maintain cell survival by trapping PUMA, and preventing its binding to other pro-survival factors such as Bcl-X_L to activate caspases. Our *in vivo* data showed that tumor cells with or without deficiency in *FBW7* and Mcl-1 degradation still grew, albeit at a slower rate, in response to 17-DMAG treatment, and tumor growth became accelerated following the last dose of treatment (Fig. 6A). These observations suggest that in addition to apoptosis, growth inhibition is also involved in the antitumor effect of Hsp90 inhibition, which may be explained by downregulation of the Hsp90 client proteins involved in regulating cell growth, such as Raf-1 and Akt (2).

Clinical applications of Hsp90 inhibitors have been hampered by lack of patient stratification due to lack of biomarkers of sensitivity and resistance (2, 5). Our findings elucidate a critical functional role of *FBW7* mutations and Mcl-1 stability in differential sensitivity and resistance of CRC cells to Hsp90 inhibition. Most of the *FBW7* mutations in CRCs are heterozygous point mutations (29). Mutant FBW7 may have altered protein stability, or act as dominant negative proteins upon hetero-dimerization with WT FBW7 (23). *FBW7* mutations are found in various human cancers and likely play a broad functional role in intrinsic and acquired therapeutic resistance of cancer cells (23). These mutations affect responses to γ-secretase inhibitors in leukemia cells (39), to HDAC inhibitors in squamous tumor cells (40), and to antimitotic drugs in CRC cells (21). Several other factors have also been shown to modulate sensitivity to Hsp90 inhibitors (41). For example, improved response rates were observed in HER2-positive metastatic breast cancer patients treated with 17-AAG and trastuzumab (42), and in ALK-rearranged non-small cell lung cancer patients treated with the Hsp90 inhibitor IPI-504 (43). These effects were attributed to the degradation of the Hsp90 clients, which are driver oncoproteins in these tumor types. Studies by us and other groups showed that *p53* mutational status influences 17-AAG sensitivity through the effects on p53 downstream targets including PUMA, Bax, Bim, and p21 (13–15). Our recent study showed that colon cancer cells contain a small fraction (~0.1%) of pre-existing *FWB7*-mutant cells, which can be enriched upon treatment with the multi-kinase inhibitor regorafenib, leading to acquired drug resistance (29). It is possible that these cells can also escape from death induced by Hsp90 inhibitors and cause acquired resistance to these agents.

Our data suggest that Mcl-1-binding BH3 mimetics are potentially useful for overcoming resistance to Hsp90 inhibitors caused by *FBW7* mutations and/or Mcl-1 stabilization in CRC cells. We recently identified a critical role of Mcl-1 and *FBW7* mutations in intrinsic and acquired resistance of CRCs to the FDA-approved multi-kinase inhibitor regorafenib (24, 29). Aberrant Mcl-1 expression is frequently detected in CRCs and significantly correlated with advanced tumor stages, lymph node metastasis, resistance to chemotherapy, and poor patient survival (44, 45). These findings suggest Mcl-1 is an attractive target for developing new anticancer agents to improve the efficacy of targeted therapies. Inhibiting pro-survival Bcl-2 family proteins in tumor cells has emerged as an attractive therapeutic strategy,

highlighted by the recent FDA approval of the Bcl-2-selective inhibitor ABT-199 (Venetoclax) for the treatment of chronic lymphocytic leukemia (46). Several different chemical classes of Mcl-1 inhibitors have been described (47, 48). The potential use of these Mcl-1 inhibitors for improving the therapeutic effects of Hsp90-targeted agents needs to be further established.

In conclusion, we demonstrate that GSK3β/FBW7-mediated Mcl-1 degradation is critical for apoptosis induce by Hsp90 inhibitors in CRC cells. Our findings suggest *FBW7* mutational status and Mcl-1 stability as key determinants of response to Hsp90 inhibitors, which provides a rationale for using *FBW7* genotype for potential patient stratification, and for drug combinations with Hsp90 inhibitors that can effectively overcome Mcl-1-mediated resistance.

Supplementary Material

Refer to Web version on PubMed Central for supplementary material.

Acknowledgments

We thank Ms. Xiao Tan for technical assistance and our lab members for critical reading and discussion.

Financial support: U.S. National Institute of Health grants R01CA172136, R01CA203028 to L Zhang; U01DK085570, U19AI068021 to J Yu; P30CA047904 to University of Pittsburgh Cancer Institute; and National Natural Science Foundation of China grant 81672942 to F Zou.

Abbreviations

17-AAG	17-allylamino-17-demethoxygeldanamycin
CRC	colorectal cancer
DAPI	4’ 6-Diamidino-2-phenylindole
17-DMAG	17-dimethylaminoethylamino-17-demethoxygeldanamycin
FBW7	F-box/WD repeat containing protein 7
5-FU	5-fluorouracil
GSK3β	glycogen synthase kinase 3β
Hsp90	heat shock protein 90
IP	immunoprecipitation
KI	knock-in
KO	knockout
MTS	3-(4,5-dimethylthiazol-2-yl)-5-(3-carboxymethoxyphenyl)-2-(4-sulfophenyl)-2H-tetrazolium
NSA	necrosulfonamide

RT-PCR	reverse transcriptase-polymerase chain reaction
Mcl-1	myeloid cell leukemia 1
siRNA	small interfering RNA
TUNEL	terminal deoxynucleotidyl transferase mediated dUTP nick end labeling
WT	wild-type.

References

1. Jarosz DF, Lindquist S. Hsp90 and environmental stress transform the adaptive value of natural genetic variation. Science. 2010; 330:1820–4. [PubMed: 21205668]
2. Neckers L, Workman P. Hsp90 molecular chaperone inhibitors: are we there yet? Clinical Cancer Research. 2012; 18:64–76. [PubMed: 22215907]
3. Hanahan D, Weinberg RA. Hallmarks of cancer: the next generation. Cell. 2011; 144:646–74. [PubMed: 21376230]
4. Butler LM, Ferraldeschi R, Armstrong HK, Centenera MM, Workman P. Maximizing the Therapeutic Potential of HSP90 Inhibitors. Mol Cancer Res. 2015; 13:1445–51. [PubMed: 26219697]
5. Hong DS, Banerji U, Tavana B, George GC, Aaron J, Kurzrock R. Targeting the molecular chaperone heat shock protein 90 (HSP90): lessons learned and future directions. Cancer Treat Rev. 2013; 39:375–87. [PubMed: 23199899]
6. Kamal A, Thao L, Sensintaffar J, Zhang L, Boehm MF, Fritz LC, et al. A high-affinity conformation of Hsp90 confers tumour selectivity on Hsp90 inhibitors. Nature. 2003; 425:407–10. [PubMed: 14508491]
7. Garg G, Khandelwal A, Blagg BS. Anticancer Inhibitors of Hsp90 Function: Beyond the Usual Suspects. Advances in cancer research. 2016; 129:51–88. [PubMed: 26916001]
8. Ghosh S, Shinogle HE, Garg G, Vielhauer GA, Holzbeierlein JM, Dobrowsky RT, et al. Hsp90 C-terminal inhibitors exhibit antimigratory activity by disrupting the Hsp90alpha/Aha1 complex in PC3-MM2 cells. ACS chemical biology. 2015; 10:577–90. [PubMed: 25402753]
9. Hostein I, Robertson D, DiStefano F, Workman P, Clarke PA. Inhibition of signal transduction by the Hsp90 inhibitor 17-allylamino-17-demethoxygeldanamycin results in cytostasis and apoptosis. Cancer Res. 2001; 61:4003–9. [PubMed: 11358818]
10. Munster PN, Marchion DC, Basso AD, Rosen N. Degradation of HER2 by ansamycins induces growth arrest and apoptosis in cells with HER2 overexpression via a HER3, phosphatidylinositol 3'-kinase-AKT-dependent pathway. Cancer Res. 2002; 62:3132–7. [PubMed: 12036925]
11. Rakitina TV, Vasilevskaya IA, O'Dwyer PJ. Additive interaction of oxaliplatin and 17-allylamino-17-demethoxygeldanamycin in colon cancer cell lines results from inhibition of nuclear factor kappaB signaling. Cancer Res. 2003; 63:8600–5. [PubMed: 14695170]
12. Davenport EL, Moore HE, Dunlop AS, Sharp SY, Workman P, Morgan GJ, et al. Heat shock protein inhibition is associated with activation of the unfolded protein response pathway in myeloma plasma cells. Blood. 2007; 110:2641–9. [PubMed: 17525289]
13. Ayrault O, Godeny MD, Dillon C, Zindy F, Fitzgerald P, Roussel MF, et al. Inhibition of Hsp90 via 17-DMAG induces apoptosis in a p53-dependent manner to prevent medulloblastoma. Proc Natl Acad Sci U S A. 2009; 106:17037–42. [PubMed: 19805107]
14. Vaseva AV, Yallowitz AR, Marchenko ND, Xu S, Moll UM. Blockade of Hsp90 by 17AAG antagonizes MDMX and synergizes with Nutlin to induce p53-mediated apoptosis in solid tumors. Cell death & disease. 2011; 2:e156. [PubMed: 21562588]
15. He K, Zheng X, Zhang L, Yu J. Hsp90 inhibitors promote p53-dependent apoptosis through PUMA and Bax. Mol Cancer Ther. 2013; 12:2559–68. [PubMed: 23966620]
16. Youle RJ, Strasser A. The BCL-2 protein family: opposing activities that mediate cell death. Nat Rev Mol Cell Biol. 2008; 9:47–59. [PubMed: 18097445]

17. Fulda S. Targeting apoptosis for anticancer therapy. Semin Cancer Biol. 2015; 31:84–8. [PubMed: 24859747]
18. Thomas LW, Lam C, Edwards SW. Mcl-1; the molecular regulation of protein function. FEBS Lett. 2010; 584:2981–9. [PubMed: 20540941]
19. Mojsa B, Lassot I, Desagher S. Mcl-1 ubiquitination: unique regulation of an essential survival protein. Cells. 2014; 3:418–37. [PubMed: 24814761]
20. Inuzuka H, Shaik S, Onoyama I, Gao D, Tseng A, Maser RS, et al. SCF(FBW7) regulates cellular apoptosis by targeting MCL1 for ubiquitylation and destruction. Nature. 2011; 471:104–9. [PubMed: 21368833]
21. Wertz IE, Kusam S, Lam C, Okamoto T, Sandoval W, Anderson DJ, et al. Sensitivity to antitubulin chemotherapeutics is regulated by MCL1 and FBW7. Nature. 2011; 471:110–4. [PubMed: 21368834]
22. Rajagopalan H, Jallepalli PV, Rago C, Velculescu VE, Kinzler KW, Vogelstein B, et al. Inactivation of hCDC4 can cause chromosomal instability. Nature. 2004; 428:77–81. [PubMed: 14999283]
23. Davis RJ, Welcker M, Clurman BE. Tumor suppression by the Fbw7 ubiquitin ligase: mechanisms and opportunities. Cancer Cell. 2014; 26:455–64. [PubMed: 25314076]
24. Tong J, Wang P, Tan S, Chen D, Nikolovska-Coleska Z, Zou F, et al. Mcl-1 degradation is required for targeted therapeutics to eradicate colon cancer cells. Cancer Res. 2017; 77:2512–21. [PubMed: 28202514]
25. Coghlan MP, Culbert AA, Cross DA, Corcoran SL, Yates JW, Pearce NJ, et al. Selective small molecule inhibitors of glycogen synthase kinase-3 modulate glycogen metabolism and gene transcription. Chemistry & biology. 2000; 7:793–803. [PubMed: 11033082]
26. Abulwerdi F, Liao C, Liu M, Azmi AS, Aboukameel A, Mady AS, et al. A novel small-molecule inhibitor of mcl-1 blocks pancreatic cancer growth in vitro and in vivo. Mol Cancer Ther. 2014; 13:565–75. [PubMed: 24019208]
27. Abulwerdi FA, Liao C, Mady AS, Gavin J, Shen C, Cierpicki T, et al. 3-Substituted-N-(4-hydroxynaphthalen-1-yl)arylsulfonamides as a novel class of selective Mcl-1 inhibitors: structure-based design, synthesis, SAR, and biological evaluation. J Med Chem. 2014; 57:4111–33. [PubMed: 24749893]
28. Peng R, Tong JS, Li H, Yue B, Zou F, Yu J, et al. Targeting Bax interaction sites reveals that only homo-oligomerization sites are essential for its activation. Cell Death Differ. 2013; 20:744–54. [PubMed: 23392123]
29. Tong J, Tan S, Zou F, Yu J, Zhang L. FBW7 mutations mediate resistance of colorectal cancer to targeted therapies by blocking Mcl-1 degradation. Oncogene. 2017; 36:787–96. [PubMed: 27399335]
30. Dudgeon C, Peng R, Wang P, Sebastiani A, Yu J, Zhang L. Inhibiting oncogenic signaling by sorafenib activates PUMA via GSK3beta and NF-kappaB to suppress tumor cell growth. Oncogene. 2012; 31:4848–58. [PubMed: 22286758]
31. Maurer U, Charvet C, Wagman AS, Dejardin E, Green DR. Glycogen synthase kinase-3 regulates mitochondrial outer membrane permeabilization and apoptosis by destabilization of MCL-1. Mol Cell. 2006; 21:749–60. [PubMed: 16543145]
32. Ding Q, Xia W, Liu JC, Yang JY, Lee DF, Xia J, et al. Erk associates with and primes GSK-3beta for its inactivation resulting in upregulation of beta-catenin. Mol Cell. 2005; 19:159–70. [PubMed: 16039586]
33. Danial NN, Korsmeyer SJ. Cell death. Critical control points. Cell. 2004; 116:205–19. [PubMed: 14744432]
34. Varadarajan S, Vogler M, Butterworth M, Dinsdale D, Walensky LD, Cohen GM. Evaluation and critical assessment of putative MCL-1 inhibitors. Cell Death Differ. 2013; 20:1475–84. [PubMed: 23832116]
35. Zhong Q, Gao W, Du F, Wang X. Mule/ARF-BP1, a BH3-only E3 ubiquitin ligase, catalyzes the polyubiquitination of Mcl-1 and regulates apoptosis. Cell. 2005; 121:1085–95. [PubMed: 15989957]

36. Ding Q, He X, Hsu JM, Xia W, Chen CT, Li LY, et al. Degradation of Mcl-1 by beta-TrCP mediates glycogen synthase kinase 3-induced tumor suppression and chemosensitization. Mol Cell Biol. 2007; 27:4006–17. [PubMed: 17387146]
37. Schwickart M, Huang X, Lill JR, Liu J, Ferrando R, French DM, et al. Deubiquitinase USP9X stabilizes MCL1 and promotes tumour cell survival. Nature. 2010; 463:103–7. [PubMed: 20023629]
38. Samant RS, Clarke PA, Workman P. E3 ubiquitin ligase Cullin-5 modulates multiple molecular and cellular responses to heat shock protein 90 inhibition in human cancer cells. Proc Natl Acad Sci U S A. 2014; 111:6834–9. [PubMed: 24760825]
39. O'Neil J, Grim J, Strack P, Rao S, Tibbitts D, Winter C, et al. FBW7 mutations in leukemic cells mediate NOTCH pathway activation and resistance to gamma-secretase inhibitors. J Exp Med. 2007; 204:1813–24. [PubMed: 17646409]
40. He L, Torres-Lockhart K, Forster N, Ramakrishnan S, Greninger P, Garnett MJ, et al. Mcl-1 and FBW7 control a dominant survival pathway underlying HDAC and Bcl-2 inhibitor synergy in squamous cell carcinoma. Cancer Discovery. 2013; 3:324–37. [PubMed: 23274910]
41. Lu X, Xiao L, Wang L, Ruden DM. Hsp90 inhibitors and drug resistance in cancer: the potential benefits of combination therapies of Hsp90 inhibitors and other anti-cancer drugs. Biochem Pharmacol. 2012; 83:995–1004. [PubMed: 22120678]
42. Modi S, Stopeck A, Linden H, Solit D, Chandarlapaty S, Rosen N, et al. HSP90 inhibition is effective in breast cancer: a phase II trial of tanespimycin (17-AAG) plus trastuzumab in patients with HER2-positive metastatic breast cancer progressing on trastuzumab. Clin Cancer Res. 2011; 17:5132–9. [PubMed: 21558407]
43. Sequist LV, Gettinger S, Senzer NN, Martins RG, Janne PA, Lilenbaum R, et al. Activity of IPI-504, a novel heat-shock protein 90 inhibitor, in patients with molecularly defined non-small-cell lung cancer. J Clin Oncol. 2010; 28:4953–60. [PubMed: 20940188]
44. Henderson-Jackson EB, Helm J, Ghayouri M, Hakam A, Nasir A, Leon M, et al. Correlation between Mcl-1 and pAKT protein expression in colorectal cancer. International journal of clinical and experimental pathology. 2010; 3:768–74. [PubMed: 21151390]
45. Lee WS, Park YL, Kim N, Oh HH, Son DJ, Kim MY, et al. Myeloid cell leukemia-1 is associated with tumor progression by inhibiting apoptosis and enhancing angiogenesis in colorectal cancer. American journal of cancer research. 2015; 5:101–13. [PubMed: 25628923]
46. Del Poeta G, Postorino M, Pupo L, Del Principe MI, Dal Bo M, Bittolo T, et al. Venetoclax: Bcl-2 inhibition for the treatment of chronic lymphocytic leukemia. Drugs of today. 2016; 52:249–60. [PubMed: 27252989]
47. Belmar J, Fesik SW. Small molecule Mcl-1 inhibitors for the treatment of cancer. Pharmacol Ther. 2015; 145:76–84. [PubMed: 25172548]
48. Kotschy A, Szlavik Z, Murray J, Davidson J, Maragno AL, Le Toumelin-Braizat G, et al. The MCL1 inhibitor S63845 is tolerable and effective in diverse cancer models. Nature. 2016; 538:477–82. [PubMed: 27760111]

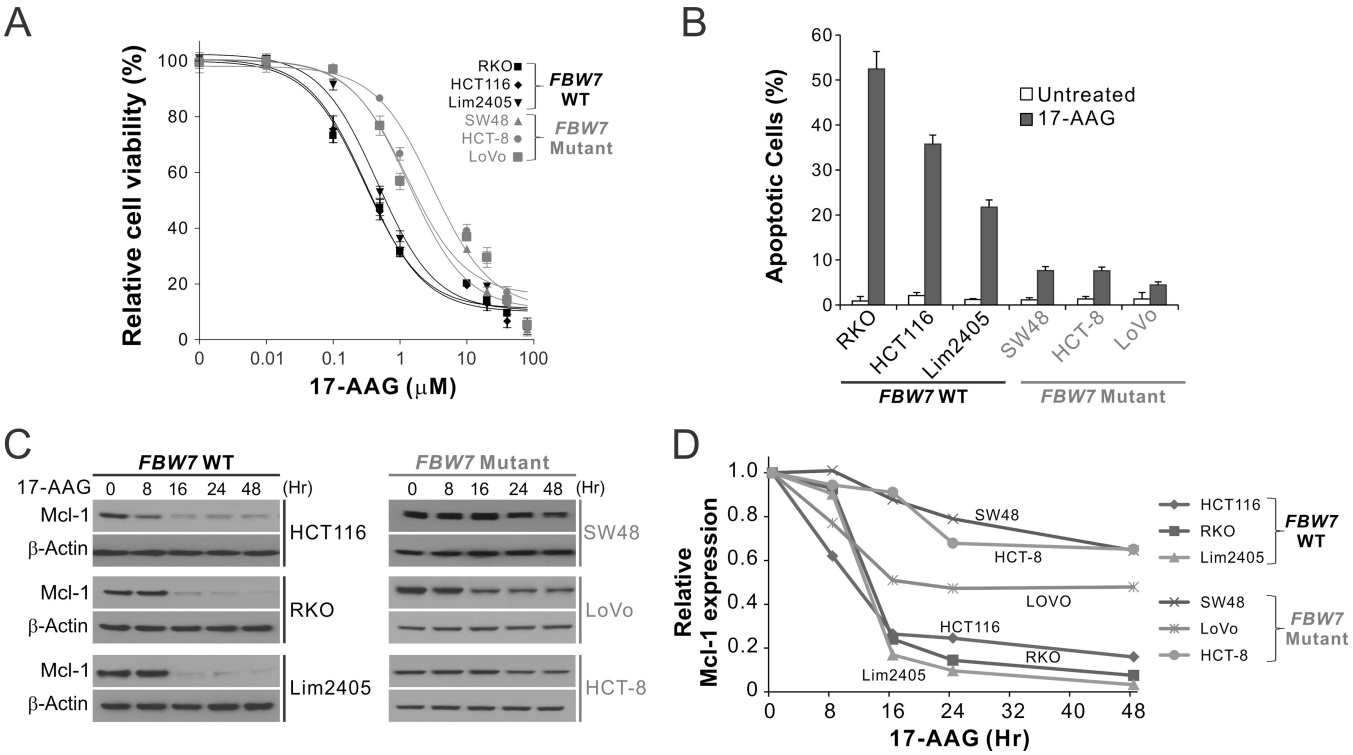

Figure 1. *FBW7*-mutant CRC cells are insensitive to Hsp90 inhibitors and lack Mcl-1 degradation

(A) MTS analysis of indicated *FBW7*-WT and -mutant CRC cell lines treated with 17-AAG at different concentrations for 72 hr. Results were expressed as means ± s.d. of three independent experiments. **(B)** Indicated *FBW7*-WT and -mutant CRC cell lines were treated with 1 μM 17-AAG for 72 hr. Apoptosis was analyzed by counting condensed and fragmented nuclei after nuclear staining. **(C)** Western blotting of Mcl-1 in indicated *FBW7*-WT and -mutant CRC cell lines treated with 1 μM 17-AAG at indicated time points. **(D)** Mcl-1 signals from (C) were quantified by the NIH Image J program, normalized to that of β-actin, and expressed as a ratio relative to untreated controls.

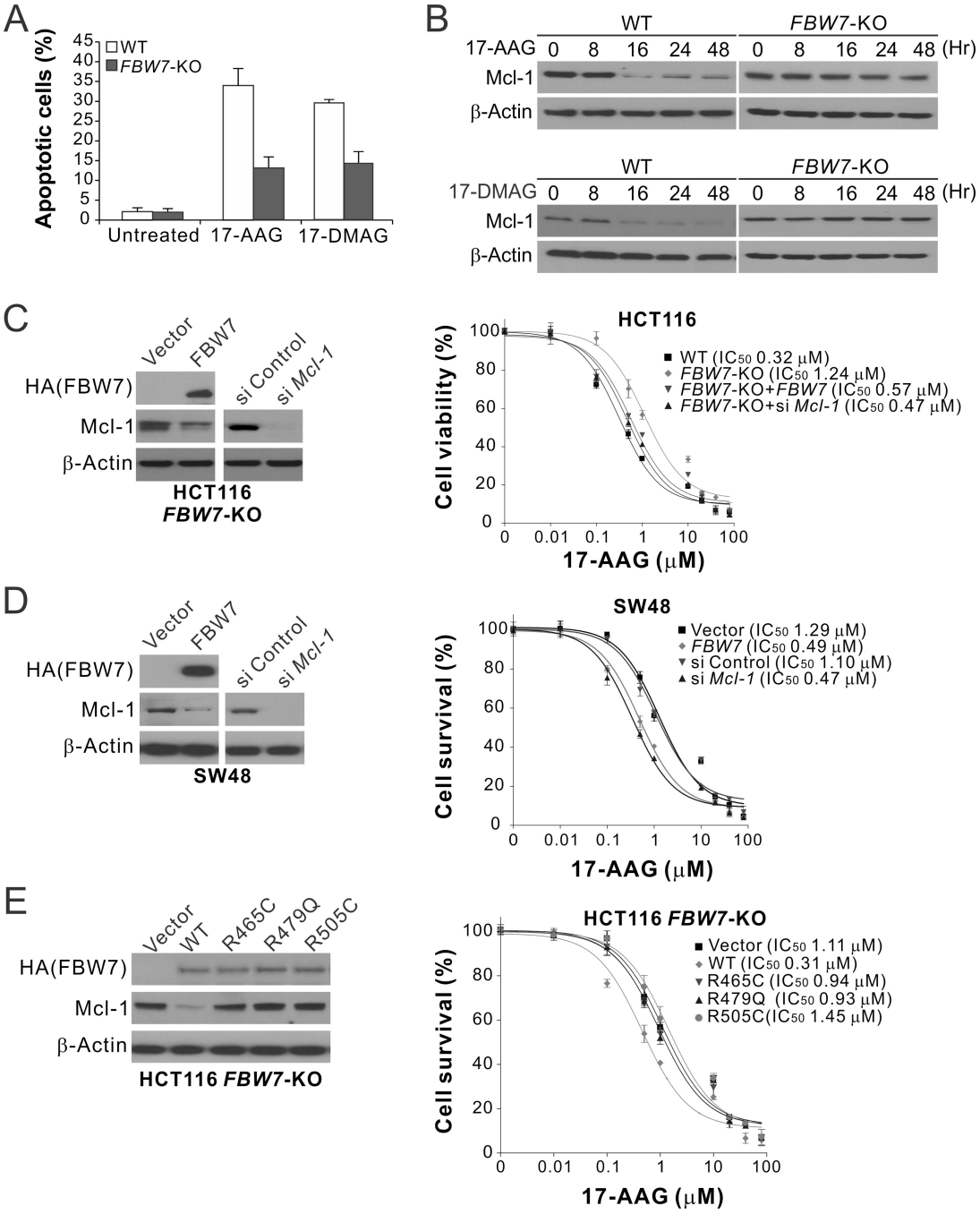

Figure 2. FBW7 is critical for cell death and Mcl-1 degradation induced by Hsp90 inhibitors in CRC cells

(A) WT and *FBW7*-KO HCT116 cells treated with 1 μM 17-AAG for 48 hr were analyzed for apoptosis by counting condensed and fragmented nuclei. **(B)** Western blotting of Mcl-1 in WT and *FBW7*-KO HCT116 cells treated with 1 μM 17-AAG or 0.25 μM 17-DMAG at indicated time points. **(C)** 17-AAG sensitivity of WT and *FBW7*-KO HCT116 cells with or without HA-tagged FBW7 transient transfection or *Mcl-1* knockdown, which was analyzed by western blotting (left panel). **(D)** 17-AAG sensitivity of *FBW7*-mutant SW48 cells with

or without HA-tagged FBW7 transient transfection or *Mcl-1* knockdown, which was analyzed by western blotting (left panel). **(E)** 17-AAG sensitivity of *FBW7*-KO HCT116 cells transiently transfected with HA-tagged WT FBW7 or indicated mutants (R465C, R479Q or R505C). Transfected FBW7 was analyzed by western blotting (left panel). In (C)–(E), 17-AAG sensitivity was analyzed by MTS assay on cells treated with 17-AAG at indicated concentrations for 72 hr. Western blotting was performed on untreated cells at 24 hr after transfection. Results in (A) and (C)–(E) were expressed as means ± s.d. of three independent experiments.

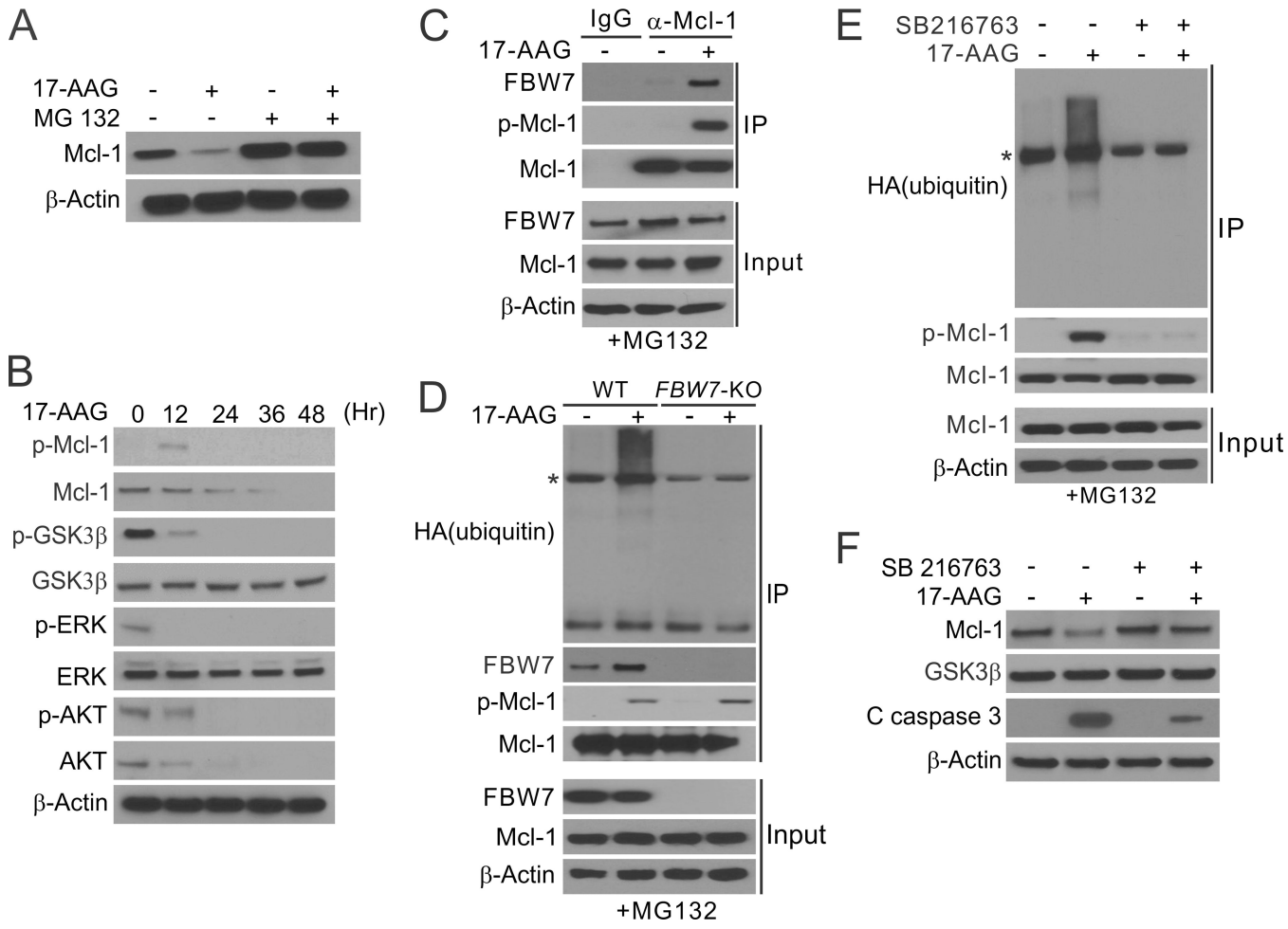

Figure 3. Hsp90 inhibition promotes GSK3β-mediated Mcl-1 phosphorylation, and its subsequent ubiquitination by FBW7 and degradation

(A) Western blotting of Mcl-1 in HCT116 cells treated with 1 μM 17-AAG for 24 hr, with or without pretreatment with 5 μM MG132 for 30 min. **(B)** Western blotting of indicated proteins in HCT116 cells treated with 1 μM 17-AAG at indicated time points. p-Mcl-1: Ser159/Thr163; p-ERK: Thr202/Tyr204; p-GSK3β: Ser9; p-AKT: Ser473. **(C)** HCT116 cells pretreated with 5 μM of the proteasome inhibitor MG132 for 30 min were treated with 1 μM 17-AAG for 24 hr. Immunoprecipitation (IP) was performed to pull down Mcl-1, followed by western blotting of indicated proteins. **(D)** WT and *FBW7*-KO HCT116 cells transfected with HA-ubiquitin and pretreated with 5 μM MG132 for 30 min were treated with 1 μM 17-AAG for 24 hr. IP was performed to pull down Mcl-1, followed by western blotting of indicated proteins. * indicates non-specific bands. **(E)** HCT116 cells transfected with HA-ubiquitin and pretreated with 5 μM of MG132 for 30 min were treated with 1 μM 17-AAG with or without the GSK3 inhibitor SB216763 for 4 hr. IP was performed to pull down Mcl-1, followed by western blotting of indicated proteins. * indicates non-specific bands. **(F)** Western blotting of indicated proteins in HCT116 cells treated with 1 μM 17-AAG alone or in combination with SB216763 for 48 hr.

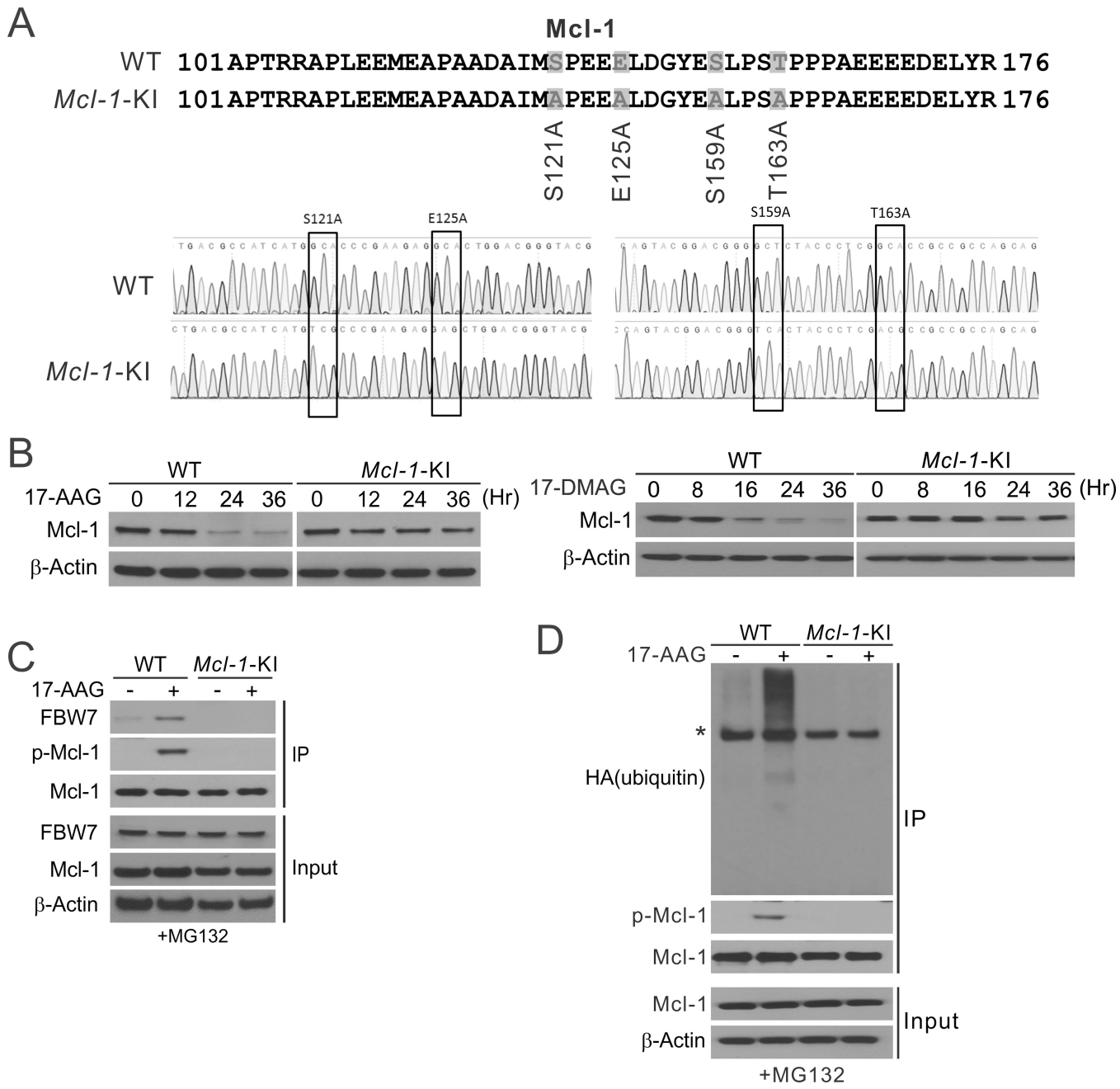

Figure 4. Mcl-1 ubiquitination and degradation induced by Hsp90 inhibitors require site specific phosphorylation

(A) *Upper*, schematic diagram of Mcl-1 phosphorylation sites in WT and HCT116 cells with Mcl-1 mutant knock-in (*Mcl-1*-KI); *lower*, sequence of the Mcl-1 genomic region in WT and *Mcl-1*-KI HCT116 cells. **(B)** Western blotting of Mcl-1 in WT and *Mcl-1*-KI HCT116 cells treated with 1 μM 17-AAG or 0.25 μM 17-DMAG at indicated time points. **(C)** WT and *Mcl-1*-KI HCT116 cells pretreated with 5 μM MG132 for 30 min were treated with 1 μM 17-AAG for 24 hr. IP was used to pull down Mcl-1, followed by western blotting of indicated proteins. **(D)** WT and *Mcl-1*-KI HCT116 cells transfected with HA-ubiquitin and pretreated with 5 μM MG132 for 30 min were treated with 1 μM 17-AAG for 4 hr. IP was

used to pull down Mcl-1, followed by western blotting of indicated proteins. * indicates non-specific bands.

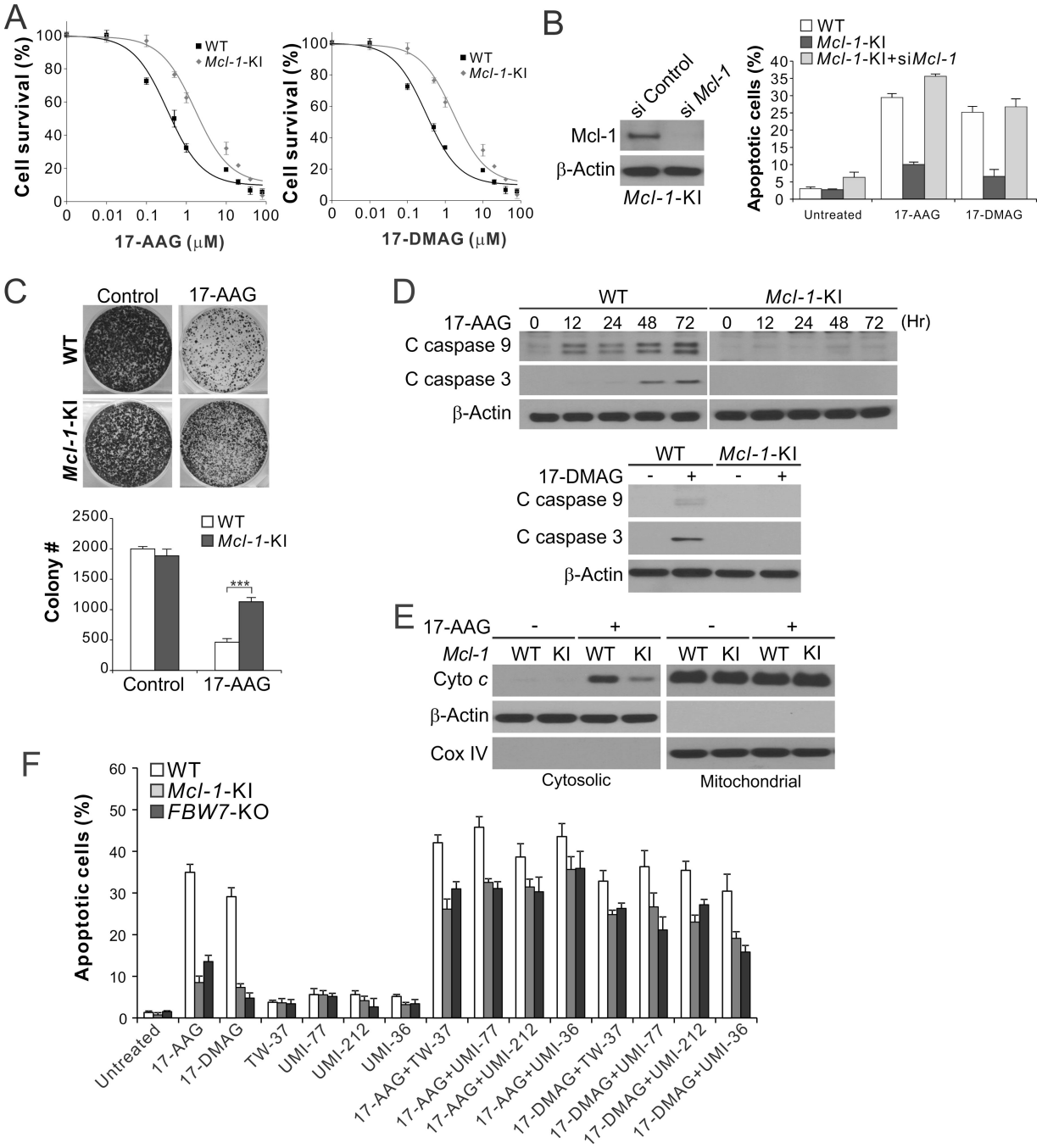

Figure 5. Blocking Mcl-1 phosphorylation and degradation suppresses 17-AAG-induced apoptosis and renders 17-AAG resistance

(A) MTS analysis of viability of WT and *Mcl-1*-KI HCT116 cells treated with 17-AAG or 17-DMAG at different concentrations for 72 hr. **(B)** Apoptosis in WT and *Mcl-1*-KI HCT116 cells with or without *Mcl-1* knockdown treated with 1 μM 17-AAG or 0.25 μM 17-DMAG for 48 hr was analyzed by nuclear staining. *Left*, western blot analysis of Mcl-1 knockdown. **(C)** Colony formation assay was done by seeding an equal number of WT and *Mcl-1*-KI HCT116 cells treated with 1 μM 17-AAG for 48 hr in 12-well plates, and staining

of the attached cells with crystal violet after 14 days. *Upper*, representative pictures of colonies; *lower*, enumeration of colony numbers. ***, $P < 0.001$. **(D)** Western blotting of cleaved (C) caspases 9 and 3 in WT and *Mcl-1* KI HCT116 cells treated with 1 μM 17-AAG or 0.25 μM 17-DMAG for 48 hr. **(E)** Cytochrome *c* release in cells treated with 1 μM 17-AAG was analyzed by western blotting of mitochondrial or cytosolic fractions isolated from treated cells. β-Actin and cytochrome oxidase subunit IV (COX IV) were used as a control for loading and fractionation. **(F)** WT, *Mcl-1*-KI and *FBW7*-KO cells were treated for 48 hr with 1 μM 17-AAG or 0.25 μM 17-DMAG alone, or in combination with 5 μM of TW-37, UMI-77, UMI-212, or UM-36. Apoptosis was analyzed by nuclear staining. In (A)–(C) and (F), results were expressed as means ± s.d. of three independent experiments.

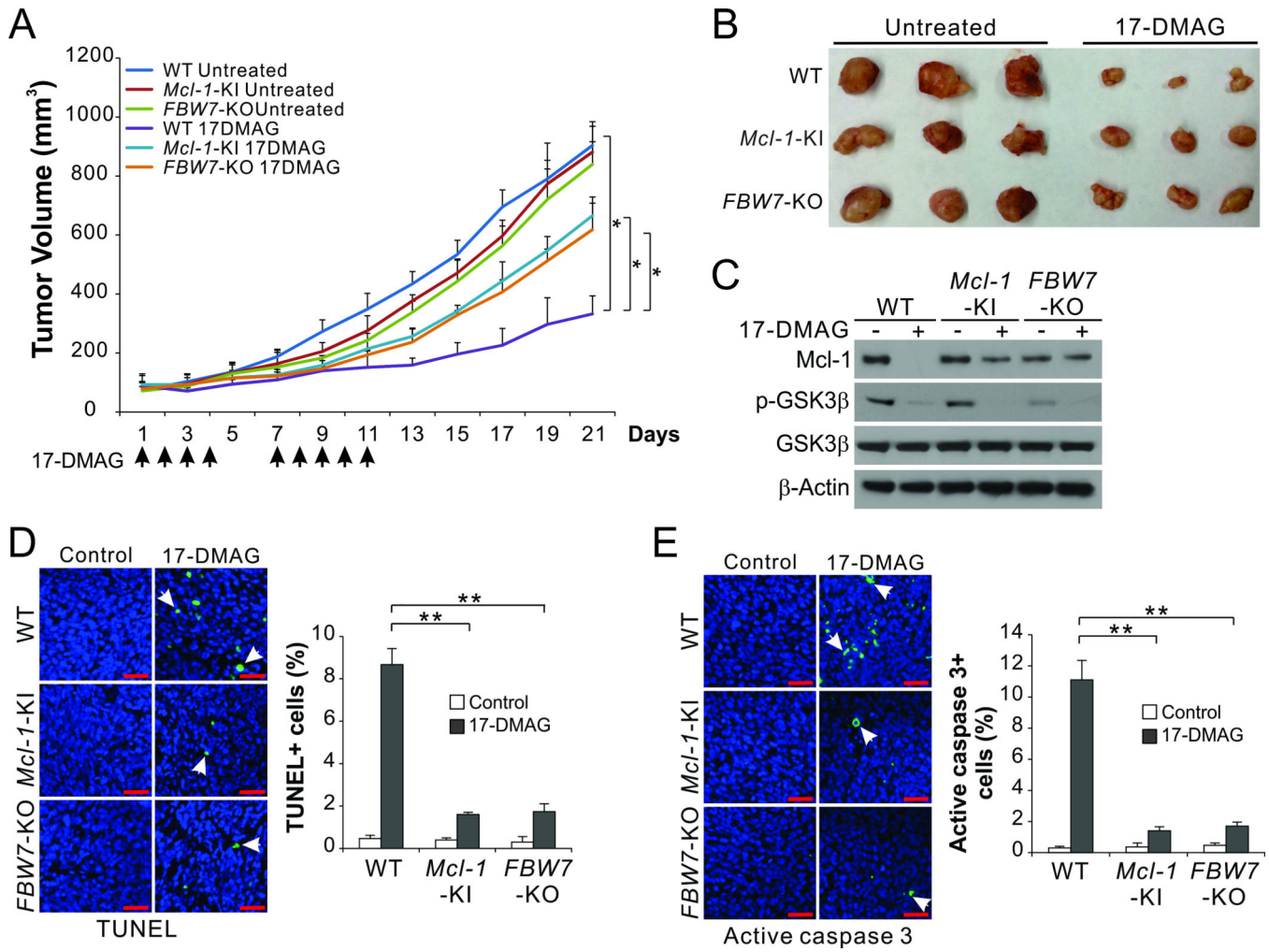

Figure 6. FBW7-mediated Mcl-1 degradation contributes to the *in vivo* antitumor activity of Hsp90 inhibition

(A) Nude mice were injected s.c. with 4×10^6 WT, *Mcl-1*-KI or *FBW*-KO HCT116 cells. After 1 week, mice were treated by intraperitoneal injection with 15 mg/kg of 17-DMAG or the control vehicle on days 1 to 4 and 7 to 11. Tumor volumes at indicated time points after treatment were measured and plotted. *, $P<0.05$; n=6 in each group. **(B)** Representative tumors at the end of the experiment. **(C)** Nude mice with WT, *Mcl-1*-KI or *FBW*-KO HCT116 tumors treated with 17-DMAG as in (A) for 5 consecutive days. Indicated proteins in randomly selected tumors were analyzed by western blotting. **(D)**, **(E)** Tissue sections from mice treated as in (C) were analyzed for apoptosis by TUNEL (D) and active caspase 3 (E) staining. *Left*, representative staining pictures with arrows indicating example cells with positive staining (scale bars, 25 μm); *right*, quantification of TUNEL and active-caspase-3-positive cell, with the results expressed as means ± s.d. of three independent experiments (**, $P<0.01$).